Quantification of edge effects in capacitive biopotential sensing*

Gautam Anand, *Member, IEEE,* Andrew Lowe, *Senior Member, IEEE,* Richard Jones, *Fellow, IEEE.*
W. Mike Arnold, *Senior Member, IEEE,* Anubha Kalra, *Member, IEEE,* Ray Simpkin, *Member, IEEE,*
Ihab Sinno, *Member, IEEE,* and David Budgett

Abstract— **Knowledge of capacitance and factors contributing to its variation is important in capacitive biopotential sensing where the dimension of the electrode is much less than the dielectric (skin). As such, this study aimed to quantify the actual capacitance exhibited by an electrode, by accounting for fringe fields (edge effects). This study simulated two different dual-electrode configurations to calculate the capacitance of each electrode in the presence and absence of the other electrode. The results were compared with existing expressions from the literature to investigate their reliability in quantifying edge effects. It was found that the capacitance expression for electrode smaller than the body shows the least difference from simulated capacitance than other expressions. However, the difference increased with increasing airgap. Also, the concentric configuration identified that the outer electrode acts as a guard to the inner electrode and can be approximated with minimum error. This will help estimate the actual effective electrode capacitance in single and multi-electrode systems and allow for efficient measurement circuit design and optimal signal processing of the biopotential of interest.**

I. Introduction

Physiological monitoring is common practice throughout healthcare and rehabilitation, sports and fitness, and desirable in consumer entertainment and industrial markets. Traditional sensors that use "wet electrodes" require time-consuming skin preparation (e.g. shaving) and adhesives that commonly cause skin irritation, and fail over time [1]. Dry electrode sensors somewhat overcome these deficiencies but are dependent on consistent electrical contact [2] and hence suffer from quality and long-term use in wearable sensing. Capacitive sensing provides advantages of comfort and long-term use but still suffers from the problems of continuously varying sensor-body impedance and ability to pick up very small magnitude signals [3].

Capacitive sensing relies on sensor-body interface capacitance. Unlike gel electrodes, capacitive electrodes must cope with high electrical impedance between the body and the sensor [4]. Fundamentally, we require markedly increased electrode sensitivity to biopotentials (rather than measurement circuit sensitivity [4], [5]) to improve signal-to-noise ratio. This work focused on understanding the effect of fringe fields on sensor capacitance. The objective of this study was to quantify the contribution of fringe fields for capacitive biopotential sensing in single and multi-electrode systems.

II. Theory – Fringe Field and Edge Correction

The simplest way of realizing a capacitance is through two parallel conductive plates separated by air or a dielectric material of certain thickness. The commonly used expression for a parallel plate capacitance is:

$$C_n = \varepsilon_0 \frac{A}{d} \qquad (1)$$

where C_n is the capacitance, ε_0 is the permittivity of free space, A is the cross-sectional area of the plates and d is the dielectric separation. For a dielectric with a relative permittivity of K, the capacitance is KC_n. C_n represents the capacitance calculated with a uniform distribution of surface charge density on the conductive plates where the electric field extends directly from one plate to another as straight lines. This expression assumes both conductive plates as identical as well as the dielectric extending completely within the extent of the plates. In capacitive sensing of biopotentials, the two plates (sensor and body) are not equal in size which makes the above expression not suitable to for calculating sensor capacitance. In such cases, we must account for non-uniform electric field at the edges of the plates, called fringe fields (and the effect known as fringe effect or edge effect). As fringe fields increase the overall capacitance of a sensor, it is important to measure or account for fringe effects.

Scott and Curtis (1939) [6] experimented to account for edge correction in circular and rectangular parallel plate capacitors.
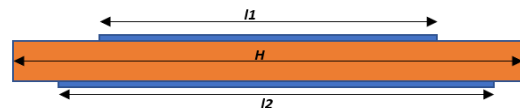

Fig. 1. Parallel plate capacitance representation with unequal conductive plates and dielectric extents.

They deduced that the capacitance between two parallel plates is composed of C_n and C_e (edge capacitance).

For circular electrodes of same size, the capacitances can be defined as:

$$C_n = \frac{1.113\, D^2}{16\, b}\ pF \qquad (2)$$

$$C_e = \frac{1.113\, D}{8\, \pi}\left[ln\frac{8\, \pi D}{b} - 3 + z\right]\ pF \qquad (3)$$

where, D is the diameter (cm), b is the dielectric thickness (cm), $z = \left(1 + \frac{t}{b}\right)ln\left(1 + \frac{t}{b}\right) - \frac{t}{b}ln\left(\frac{t}{b}\right)$, and t is the thickness of each electrode (cm).

If the extents of the two plates are *l1* and *l2* and that of the dielectric medium is H (Fig. 1), Table 1 defines the effective capacitance for different cases:

Anand is with Hemideina Pty Ltd. W.M. Arnold and I. Sinno are with Callaghan Innovation, Wellington, NZ. R. Simpkin was with Callaghan Innovation, Auckland, NZ. He is now with Emrod Limited, Auckland, NZ. D. Budgett is with University of Auckland, Auckland, NZ. R. Jones is with NZ Brain Research Institute and Electrical and Computer Engineering, University of Canterbury, Christchurch, NZ.

TABLE I: Effective capacitance expressions for different cases

Condition	Effective capacitance
Case 1: $l1 = l2 = H$	K $C_n + C_e$
Case 2: $l1 = l2 < H$	K $(C_n + C_e)$
Case 3: $l1 < l2 = H$	K $(C_n + C_{e'})$; where $C_{e'} = \frac{1.113\,D}{4\,\pi}\left[ln\frac{4\,\pi D}{b} - 3 + z'\right]$ and $z' = \left(1 + \frac{t}{2b}\right)ln\left(1 + \frac{t}{2b}\right) - \frac{t}{2b}\ln\left(\frac{t}{2b}\right)$

To add to Case 3, if a driven *guard* electrode is placed around the smaller plate, it can remove the need for edge correction and the effective capacitance is given by $KC_{n'}$, where

$$C_{n'} = \frac{1.113\,(D+y)^2}{16\,b}\ pF \qquad (4)$$

and y is the gap between the guarded and guard electrodes. The width of the guard ring should be at least twice the thickness of the dielectric. This yields errors less than 1%.

III. Methodology

This investigation aimed at calculating the capacitance for single and multi-electrode systems to determine the accuracy of above formulae for edge correction. This study involved developing a capacitance model setup in Ansys® Maxwell 2018.1 simulator and solving for capacitance using the Electrostatics solver. The model was setup according to Fig. 1. The sensor electrodes were realized in two dual-electrode configurations as thin copper conductors (0.01mm thick) in contact with a dielectric with skin properties at 1.0 Hz (K = 1136, Conductivity = 0.0002 S/m) and thickness of 1.2mm. Another circular conductor (0.01 mm thick) was considered at the bottom face of the skin to mimic the voltage source (1.0 mV). The dual-electrode configurations were implemented in two ways – with two electrodes adjacent to each other and a concentric electrode configuration (Fig. 2). Both configurations had electrodes of dissimilar areas (E1 and E2). For adjacent configuration, electrode E1 had a diameter of 17.0 mm, E2 had a diameter of 5.0 mm and an inter-electrode separation of 0.5 mm. For concentric configuration, E2 retained the same diameter of 5.0 mm, but E1 was realized with an inner diameter of 6mm and outer diameter of 18.0 mm, which resulted in the same area of E1 in both configurations. The inter-electrode gap was 0.5mm. For both configurations, the source and skin were setup with diameters of 140.0 mm.

The investigation for both configurations was carried out to calculate the capacitances of each electrode with and without the other electrode. As can be seen in Fig. 2, E1 represents the electrode with a bigger area and E2 with that of a smaller area.
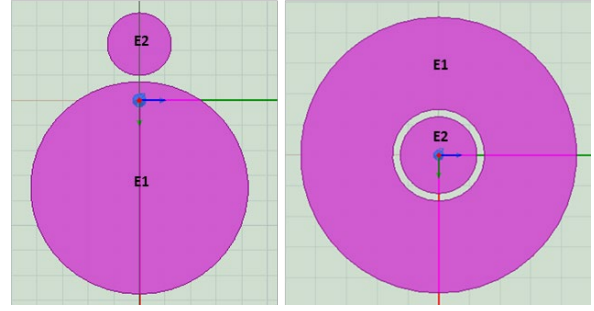

Fig. 2. Adjacent and Concentric dual-electrode configurations

The methodology involved electrostatics simulation for the following cases:

a. Calculating E1 capacitance in absence of E2, C_{E1}

b. Calculating E2 capacitance in absence of E1, C_{E2}

c. Calculating E1 capacitance with E2 present, $C_{E1}(E2)$ and E2 capacitance with E1 present, $C_{E2}(E1)$.

Steps a, b and c were repeated for both the configurations in Fig. 2. Also, the simulations were repeated for air gaps (between sensor and skin) between 0.5 to 7.0 mm in steps of 0.5mm. The simulated capacitance of electrodes was compared with the capacitance calculated with no edge correction (C_n) as in Eq. (2), and the Cases 1 – 3 in Table 1 as C_{case1}, C_{case2}, and C_{case3}, respectively.

IV. Results

A. Adjacent Configuration

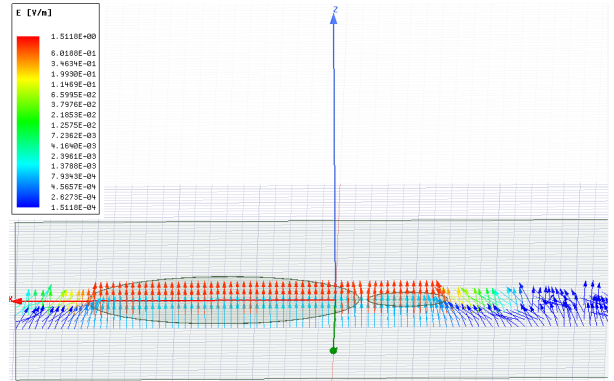Fig. 3 shows the electric field plot for E1 and E2 simulated in adjacent configuration.

Fig. 3. Electric Field Vector plot showing fringing effects in Adjacent configuration

1) Estimation of E1 capacitance

Table II shows the calculated value of E1 capacitance without E2 (C_{E1}), E1 capacitance in the presence of E2 ($C_{E1}(E2)$) and comparison with all the cases, under the condition of no air gap.

TABLE II: E1 capacitance (pF) without air gap

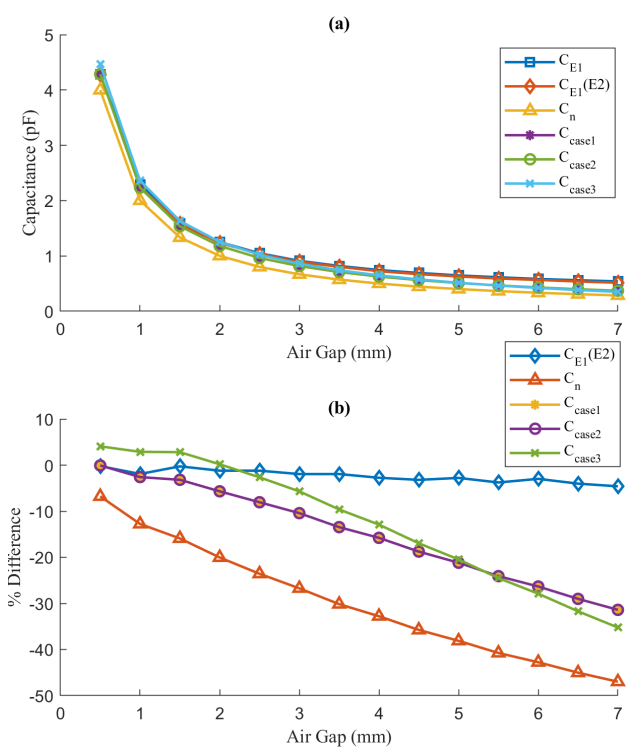| C_{E1}	$C_{E1}(E2)$	C_n	C_{case1}	C_{case2}	C_{case3}
2179.0	2167.5	1895.9	1896.7	2145.8	2273.3

1005

Fig. 4. (a) C_{E1} comparison with other cases, with varying air gaps, (b) percentage difference of C_{E1} from other cases
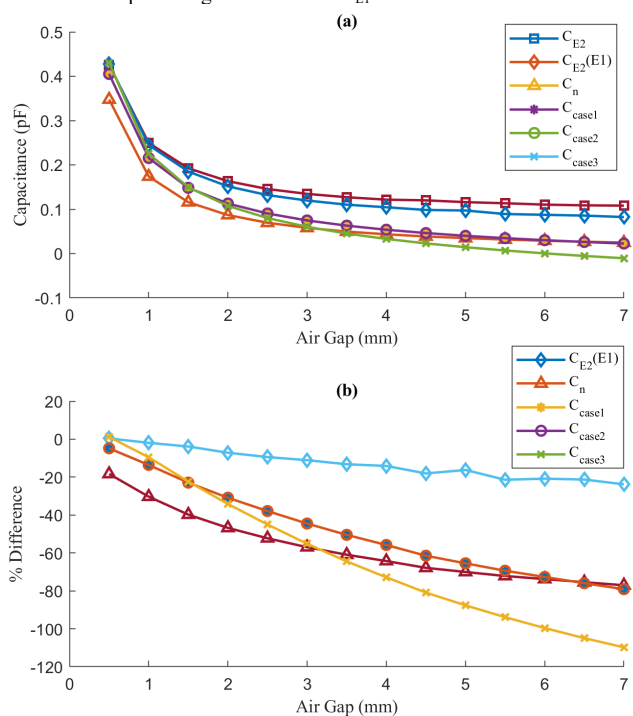

Fig. 5. (a) C_{E2} comparison with other cases, with varying air gaps, (b) percentage difference of C_{E2} from other cases

Fig. 4 (a) shows the variation of E1 capacitance with air gap, in comparison with the other cases. Also, Fig. 4(b) shows the percentage difference of C_{E1} from all other cases.

2) Estimation of E2 capacitance
Table III shows the calculated value of E2 capacitance without E1 (C_{E2}), E2 capacitance in the presence of E1 ($C_{E2}(E1)$) and comparison with all the cases, under the condition of no air gap.

TABLE III: E2 CAPACITANCE (PF) WITHOUT AIR GAP

C_{E2}	$C_{E2}(E1)$	C_n	C_{case1}	C_{case2}	C_{case3}
246.8	243.9	164.6	164.7	207.4	214.9

Fig. 5 (a) shows the variation of E2 capacitance with air gap, in comparison with the other cases. Also, Fig. 5(b) shows the percentage difference of C_{E2} from all other cases.

B. Concentric Configuration
Fig. 6 shows the electric field distribution for different cases in concentric configuration.
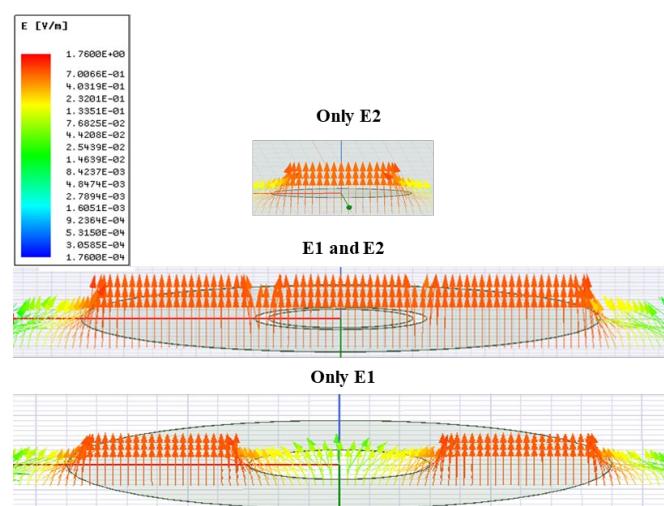

Fig. 6. Electric Field Vector plots showing fringing effects in Concentric configuration

1) Estimation of E1 capacitance
Table IV shows the calculated value of E1 capacitance without E2 (C_{E1}), E1 capacitance in the presence of E2 ($C_{E1}(E2)$) and comparison with C_n (as there are no formulae for other cases with E2 geometry) under condition of no air gap.

TABLE IV: E1 CAPACITANCE (PF) WITHOUT AIR GAP

C_{E1}	$C_{E1}(E2)$	C_n
2285.0	2219.3	1895.9

Fig. 7(a) shows C_{E1} variation with air gap and compared to $C_{E1}(E2)$ and C_n. Fig. 7(b) shows the percentage difference of C_{E1} from the other two cases.

2) Estimation of E2 capacitance
Table V shows the calculated value of E2 capacitance without E1 (C_{E2}), E2 capacitance in the presence of E1 ($C_{E2}(E1)$) and comparison with all the cases, under the condition of no air gap.

TABLE V: E2 CAPACITANCE (PF) WITHOUT AIR GAP

C_{E2}	$C_{E2}(E1)$	C_n	C_{case1}	C_{case2}	C_{case3}
246.8	193.3	164.5	164.7	207.4	214.2

Fig.8 (a) shows the variation of E2 capacitance with air gap, in comparison with the other cases. Also, Fig. 5(b) shows the percentage difference of C_{E2} from all other cases.
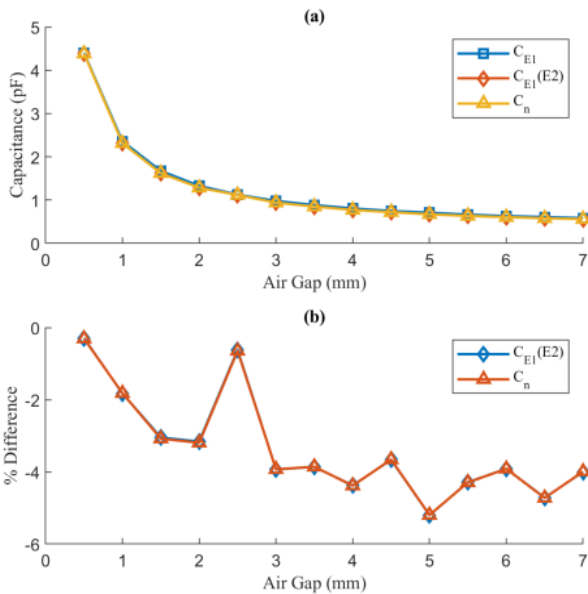
Fig. 7. (a) C_{E1} comparison with other cases, with varying air gaps, (b) percentage difference of C_{E1} from other cases
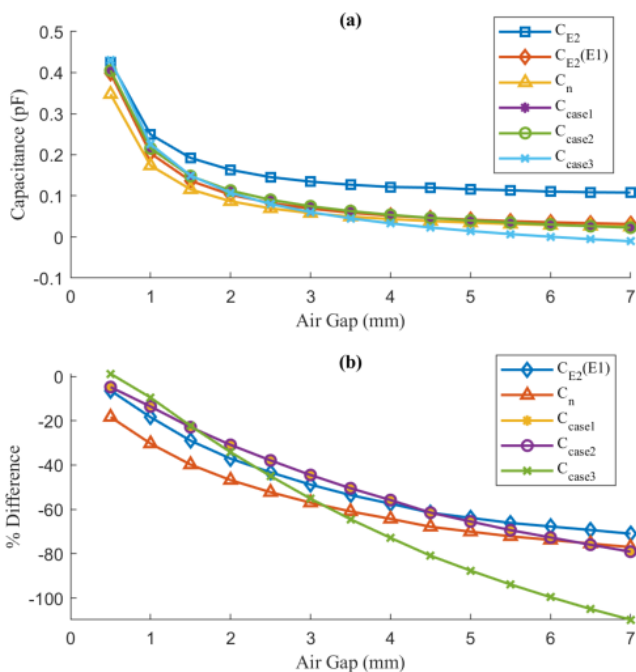

Fig. 8. (a) C_{E2} comparison with other cases, with varying air gaps, (b) percentage difference of C_{E2} from other cases

V. DISCUSSION

Different behaviours were observed in both the configurations. Generally, the calculated capacitance of the smaller electrode (E2) showed greater errors than the electrode with larger area (E1). Fringe effects were found to be more dominant in a smaller electrode due to a smaller aspect ratio (l/b) than the larger electrode. In terms of quantifying fringe effects, evaluation of the formulae proposed by Scott and Curtis [6] showed varying degrees of accuracy. In the adjacent configuration, capacitance of E1 was more closely approximated by Case 2, however, the difference increased with increasing air gap. E2 capacitance was closer to Case 3 with increasing difference with air gap. In the concentric configuration, E1 capacitance showed a

significant difference (17%) from the theoretical estimation without edge correction at no air gap. However, the difference decreased to within 6% at the maximum air gap tested. E2 capacitance, under condition of air gap, in concentric configuration was same as in the adjacent configuration except during the presence of E1 ($C_{E2}(E1)$). This value, 193.3 pF, only deviated 3% from that calculated by Eq. (4) (199.2 pF). As such, this supports that, in the concentric configuration, the outer electrode acts as a guard to the fringing caused at the inner electrode, and can be approximated by the proposed formula in Eq. (4). However, this guarding effect should be tested at different inter-electrode gaps for estimating capacitance under those cases.

VI. CONCLUSION

This work presented a simulation-based investigation into calculating the effective capacitances of electrodes, which is relevant in capacitive biopotential sensing. Two different configurations of dual-electrode setups were simulated for capacitance and compared with theoretical expressions to quantify edge effects. Overall, Case 3 (from Table I) performed the best in terms of approximating the sensor capacitance. However, all cases showed poor performance at increasing air gaps. Notably, the outer electrode in the concentric configuration was found to be, if used as a driven guard, effective in limiting the fringing of the inner electrode. However, this warrants further investigation at different electrode geometries and inter-electrode gaps. Additionally, we acknowledge that this is a simulation-based study and any conclusions should be confirmed by thorough experimental investigation. However, this work did provide an important insight into one of the factors contributing to the varying capacitances of the sensor-body interface, which contributes directly to measurement circuit design and signal processing in physiological monitoring.

REFERENCES

[1] N. Meziane, J. G. Webster, M. Attari, and A. J. Nimunkar, "Dry electrodes for electrocardiography," *Physiol. Meas.*, vol. 34, no. 9, pp. R47-69, Sep. 2013, doi: 10.1088/0967-3334/34/9/r47.

[2] B. Taji, S. Shirmohammadi, V. Groza, and I. Batkin, "Impact of skin–electrode interface on electrocardiogram measurements using conductive textile electrodes," *IEEE Trans. Instrum. Meas.*, vol. 63, no. 6, pp. 1412–1422, 2014.

[3] J. Heikenfeld *et al.*, "Wearable sensors: modalities, challenges, and prospects," *Lab. Chip*, vol. 18, no. 2, pp. 217–248, Jan. 2018, doi: 10.1039/C7LC00914C.

[4] J. Xu, S. Mitra, C. Van Hoof, R. F. Yazicioglu, and K. A. A. Makinwa, "Active Electrodes for Wearable EEG Acquisition: Review and Electronics Design Methodology," *IEEE Rev. Biomed. Eng.*, vol. 10, pp. 187–198, 2017, doi: 10.1109/RBME.2017.2656388.

[5] B. Ryan, "High Impedance Amplifiers for Non-Contact Bio-Potential Sensing," M.E. Thesis, Vic. Univ. of Wellington, Wellington, New Zealand, 2013.

[6] A. Scott and H. L. Curtis, "Edge correction in the determination of dielectric constant," *J. Res. Natl. Bur. Stand.*, vol. 22, pp. 747–775, 1939, doi: 10.6028/JRES.022.008.